Cross-Linked "Poisonous" Polymer: Thermochemically Stable Catalyst Support for Tuning Chemoselectivity

Seongho Yun,[†,#] Songhyun Lee,[†,#] Sunwoo Yook,[†] Hasmukh A. Patel,[‡] Cafer T. Yavuz,[‡] and Minkee Choi*,[†]

[†]Department of Chemical and Biomolecular Engineering, Korea Advanced Institute of Science and Technology, Daejeon 305-701, Republic of Korea

[‡]Graduate School of Energy, Environment, Water, and Sustainability (EEWS), Korea Advanced Institute of Science and Technology, Daejeon 305-701, Republic of Korea

Ⓢ *Supporting Information*

ABSTRACT: Designed catalyst poisons can be deliberately added in various reactions for tuning chemoselectivity. In general, the poisons are "transient" selectivity modifiers that are readily leached out during reactions and thus should be continuously fed to maintain the selectivity. In this work, we supported Pd catalysts on a thermochemically stable cross-linked polymer containing diphenyl sulfide linkages, which can simultaneously act as a catalyst support and a "permanent" selectivity modifier. The entire surfaces of the Pd clusters were ligated (or poisoned) by sulfide groups of the polymer

support. The sulfide groups capping the Pd surface behaved like a "molecular gate" that enabled exceptionally discriminative adsorption of alkynes over alkenes. H_2/D_2 isotope exchange revealed that the capped Pd surface alone is inactive for H_2 (or D_2) dissociation, but in the presence of coflowing acetylene (alkyne), it becomes active for H_2 dissociation as well as acetylene hydrogenation. The results indicated that acetylene adsorbs on the Pd surface and enables cooperative adsorption of H_2. In contrast, ethylene (alkene) did not facilitate H_2-D_2 exchange, and hydrogenation of ethylene was not observed. The results indicated that alkynes can induce decapping of the sulfide groups from the Pd surface, while alkenes with weaker adsorption strength cannot. The discriminative adsorption of alkynes over alkenes led to highly chemoselective hydrogenation of various alkynes to alkenes with minimal overhydrogenation and the conversion of side functional groups. The catalytic functions can be retained over a long reaction period due to the high thermochemical stability of the polymer.

KEYWORDS: hydrogenation, chemoselectivity, polymers, poison, modifier, palladium
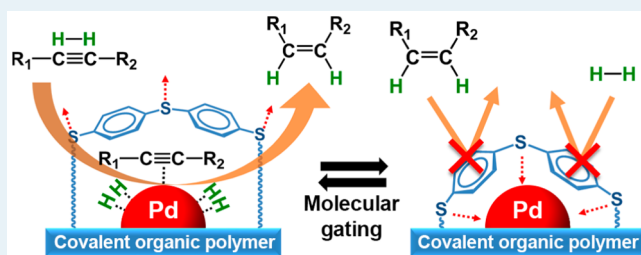
■ INTRODUCTION

Partial hydrogenation of alkynes to alkenes is an important model reaction for fundamental investigation of chemoselectivity in heterogeneous catalysis and also a key transformation in fine chemical synthesis.[1,2] Despite various efforts, development of a catalyst system simultaneously showing high selectivity and long catalyst lifetime remains a challenge. It has been demonstrated that Pd-based catalysts are the most effective choice for selective hydrogenation, although the unmodified Pd catalyst is not selective and readily forms an overhydrogenated product, alkanes. Conventional approaches for enhancing the catalytic selectivity of Pd to alkenes include alloying with secondary metals (e.g., Pb,[3−5] Cu,[5−8] Ag,[5,9−11] Au,[5,12,13] and Ga[5,14,15]), surface decoration with various metal oxide promoters,[16] and interstitial modification with C[15,17−19] and B.[20] Recently, it was also reported that single-site metal catalysts are highly selective to alkene production.[6,7,11,21]

Another important strategy is to add various modifiers (or catalyst poisons) such as carbon monoxide[22,23] and heteroatom-containing (N,[24−26] S,[27,28] P[29,30]) organic molecules

either during the catalyst preparation[24−30] or to the reactant feeds during the reaction.[22,23] These modifiers can be adsorbed on the catalyst surface in moderate strength, which modulates the adsorption/desorption behaviors of reactants/intermediates[25] or preferably poison the catalytic active sites for unselective reactions.[28] The beauty of this strategy is that, in principle, it can provide a route for precise tuning of catalytic properties, because a wide variety of modifiers having diverse molecular structures and adsorption properties can be designed via organic synthesis. On the other hand, the molecular modifiers also have a significant limitation compared to inorganic promoters. In general, the modifiers should be continuously supplied to the reaction feeds to maintain selectivity,[31] because they are readily decomposed[27] or leached out during reactions.[32,33] In other words, the molecular modifiers are not a "permanent" selectivity modifier but rather
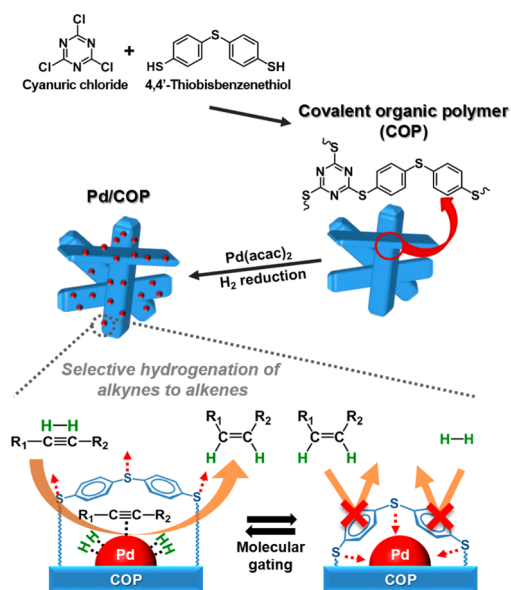
a "transient" modifier.[28] This requires continuous consumption of modifiers and additional separation steps for removing the modifiers from products.

In recent years, metal catalysts supported on organic polymers have attracted increasing attention in various catalytic reactions as a means of achieving enhanced activity, selectivity, and recyclability, compared with metal catalysts on conventional inorganic supports.[34−36] In the present work, we supported Pd catalysts on a thermochemically stable covalent organic polymer (COP) containing diphenyl sulfide linkages which can act as a permanent modifier (Scheme 1). Pd clusters

were formed on the surface of the polymer matrix, where the sulfide groups of the polymer framework can cover the entire Pd surface. The sulfide functional groups capping the Pd surface behave like a "molecular gate" that enables exceptionally discriminative adsorption of alkynes over alkenes. This leads to highly selective partial hydrogenation of various alkynes to alkenes with minimal conversion of other functional groups. Due to the high thermochemical stability and suppressed coke formation, the catalyst retains its catalytic functions during acetylene hydrogenation at 393 K over a long period (≫15 days). The result indicates that the COP simultaneously acts as a stable catalyst support and a permanent selectivity modifier.

Scheme 1. Synthesis of Pd Catalyst Supported on a Covalent Organic Polymer (COP) and Its Selective Alkyne-to-Alkene Hydrogenation Mechanism

■ RESULTS AND DISCUSSION

The COP was synthesized by a single-step nucleophilic substitution of cyanuric chloride with 4,4′-thiobisbenzenethiol (Scheme 1), following a modified version of a procedure reported elsewhere.[37] Namely, we modified the polymer synthesis conditions to maximize the surface area of the essentially nonporous polymer (Figure S1),[37] thereby making the material more suitable as a catalyst support. It appears that the polymer morphology is highly sensitive to solvent polarity, and a polymer having a nanoneedle morphology (Figure 1a) can be synthesized by using cyclohexanone as a solvent. The COP showed several well-distinguished XRD peaks (Figure S2) that indicates crystallinity, although earlier work reported a completely amorphous nature for this polymer.[37] The result implies that solvent polarity significantly affects the rate of polymerization and self-assembling rate of growing polymer chains which determine the crystallinity of the resultant polymer framework. The unique nanoneedle morphology appears to have originated from the crystalline framework nature. According to N_2 adsorption−desorption at 77 K (Figure S1), the resultant polymer exhibited a BET surface area of 55 m^2 g^{-1} and only the presence of interparticular macroporosity (pore volume: 0.53 mL g^{-1}). Elemental analysis revealed that the polymer contains 9.1 wt % N and 31 wt % S,
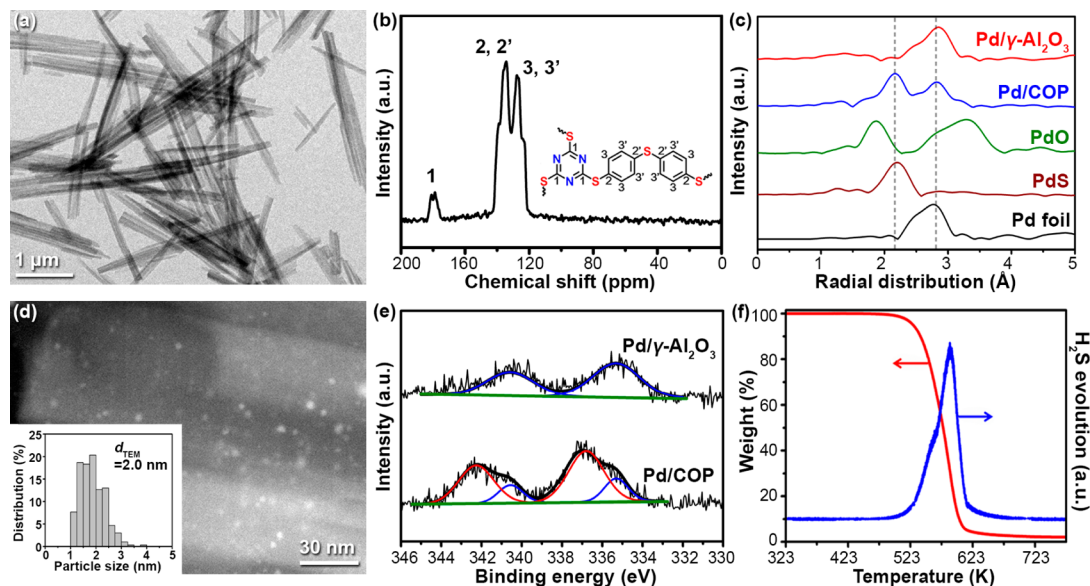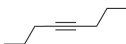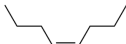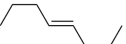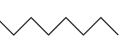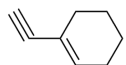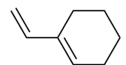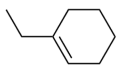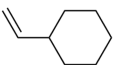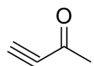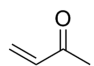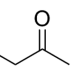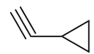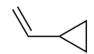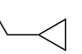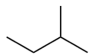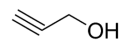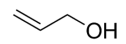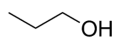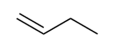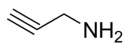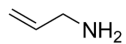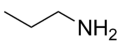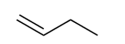

Figure 1. (a) TEM image and (b) solid-state CP/MAS ^{13}C NMR spectrum of COP. (c) Fourier transforms of k^3-weighted Pd K-edge EXAFS of Pd/γ-Al$_2$O$_3$, Pd/COP, PdO, PdS, and Pd foil. (d) HAADF-STEM image of Pd/COP. The inset shows a histogram of particle size distribution for Pd. Surface-area-weighted cluster diameter, d_{TEM}, was calculated from $\bar{d}_{TEM} = \Sigma n_i d_i^3 / \Sigma n_i d_i^2$. (e) XPS-Pd (3d) spectra of Pd/COP and Pd/γ-Al$_2$O$_3$. (f) Weight loss and H$_2$S evolution of Pd/COP during temperature ramping under H$_2$, which were measured with TGA-MS.

Table 1. Hydrogenation of Various Alkyne Compounds over Pd/COP and Pd/γ-Al₂O₃

Reaction	Reactant conversion (%)	TOR[a] (mol$_{reactant}$ mol$_{Pd}^{-1}$ sec^{-1})	Product selectivity (%)				
1							etc.
Pd/COP	89.9	0.18	85.6	9.0	1.8	3.6	
Pd/γ-Al₂O₃	89.8	2.69	37.4	18.4	14.9	29.2	
2							etc.
Pd/COP	96.3	0.19	85.1	10.1	2.8	0.4	1.6
Pd/γ-Al₂O₃	97.1	0.97	20.3	56.1	8.2	6.1	9.3
3							
Pd/COP	96.1	0.19	89.0	11.0			
Pd/γ-Al₂O₃	97.6	0.98	42.5	57.5			
4							etc.
Pd/COP	93.9	0.19	93.7	5.0	0.1	1.2	
Pd/γ-Al₂O₃	93.8	0.94	21.6	61.2	11.4	5.8	
5							
Pd/COP	95.3	0.19	91.9	4.2	3.5	0.4	
Pd/γ-Al₂O₃	98.4	0.98	12.4	45.8	39.4	2.4	
6							
Pd/COP	89.0	0.04	94.3	5.1	0.6	0.0	
Pd/γ-Al₂O₃	88.5	0.89	40.8	58.2	1.0	0.0	

[a]Catalytic turnover rate (TOR) was calculated on the basis of the total number of Pd rather than that of the accessible surface Pd determined by H₂ or CO chemisorption. This is because Pd/COP showed almost zero H/Pd and CO/Pd values in chemisorptions, which led to a scientifically meaningless TOR value of "infinity" for the latter definition.

which are very close to the theoretically predicted values (9.3 wt % N and 32 wt % S). CP/MAS ^{13}C NMR spectrum showed three peaks, which can be assigned to triazine ring carbons (179 ppm) and aromatic benzene ring carbons (134 and 128 ppm), respectively (Figure 1b).

Pd catalysts were supported on the COP by wet impregnation of Pd(acac)₂ in THF solution, followed by H₂ reduction at 453 K. ICP-MS analysis revealed that Pd content is 1.2 wt %. High-angle annular dark field scanning transmission electron microscopy (HAADF-STEM) revealed that Pd clusters having an average diameter of ca. 2.0 nm were dispersed on the polymer support (Figure 1d and S3). No characteristic peak for Pd^0 was observed in the XRD pattern of Pd/COP (Figure S2), which also supports the predominant presence of highly dispersed small Pd clusters. The radial distribution functions obtained from the k^3-weighted Pd K-edge extended X-ray absorption fine structure (EXAFS) showed that the catalyst possesses substantial Pd–S coordination (CN: 2.67) at 2.33 Å along with Pd–Pd coordination (CN: 7.01) at 2.78 Å (Figure 1c and Table S1 in the Supporting Information). The substantial Pd–S coordination indicated that the surface of the Pd catalyst is ligated with the sulfur moieties of the polymer framework. Since double-shell EXAFS fitting with Pd–Pd and Pd–S scattering shells already provided a good fitting result (R factor: 0.004), we could not find any strong evidence proving the interaction between Pd and the nitrogen groups of the triazine rings of COP in EXAFS (Pd–N bond length is

reported to be 2.05 Å[38]). We believe that the triazine ring is mainly functioning as a building block for cross-linked polymer, whereas the sulfur groups of 4,4′-thiobisbenzenethiol are predominantly interacting with the Pd surface, as shown in Scheme 1. On the other hand, a conventional Pd/γ-Al₂O₃ catalyst prepared for comparison predominantly showed Pd–Pd coordination (CN: 10.4) (Figure 1c).

XPS for Pd (3d) (Figure 1e) were deconvoluted by assuming that a signal for an individual species comprises 3d$_{3/2}$ and 3d$_{5/2}$ peaks with an intensity ratio of 2:3, which are separated by an energy difference of 5.26 eV.[39] In the case of Pd/COP, the 3d$_{5/2}$ peak at a binding energy of 335.3 eV indicates the presence of metallic Pd (Pd^0).[39] The more intense peak at 337.1 eV represents Pd^{2+}–S species.[40] On the other hand, Pd/γ-Al₂O₃ showed a major peak at a binding energy of 335.3 eV, which represents Pd^0 species.

In order to analyze the surface accessibility of the supported Pd catalysts, H₂ and CO chemisorption experiments were carried out. The results showed that Pd/COP cannot adsorb H₂ or CO on the surface of Pd clusters (H/Pd ≪0.01; CO/Pd ≪0.01). In contrast, Pd/γ-Al₂O₃ catalyst showed appreciable chemisorption amounts for both gas titrants (H/Pd = 0.53; CO/Pd = 0.58). The results reveal that the entire surface of the Pd clusters in Pd/COP is ligated (or poisoned) with the diphenyl sulfide-like moieties of the polymer matrix, and thus, no clean Pd surface is accessible to H₂ and CO. Considering the fact that Pd was supported on the surface of premade

nonporous COP particles, it is remarkable that the entire Pd surface is decorated with a sulfur-containing polymer framework, which resulted in zero chemisorption of H_2 and CO. We believe that the organic COP framework has at least some flexibility, and thus, the polymer framework nearby supported Pd clusters can cover the Pd surface to maximize the strong interaction between sulfur moieties and Pd during the catalyst preparation. This is conceptually analogous to the "strong metal−support interaction (SMSI)" often found in metal catalysts supported on inorganic metal oxide supports.[41−43]

Conventional organic polymers generally show very low thermochemical stability and thus have been considered to be unsuitable as catalytic materials for reactions at elevated temperatures (>373 K). In this sense, it is remarkable that the present COP possesses extra-high thermal stability up to 673 K under an inert atmosphere due to its highly cross-linked aromatic structure.[37] Nevertheless, thermochemical stability under catalytically relevant conditions (i.e., in the presence of embedded Pd catalysts and a H_2 atmosphere) may be significantly lower than the one under inert gas, because Pd under H_2 can catalyze hydrodesulfurization and hydrogenolysis of the polymer framework. With this regard, we carried out a thermogravimetric analyzer-mass spectrometer (TGA-MS) analysis of Pd/COP under H_2 (Figure 1f). The result shows that polymer decomposition starts at ∼503 K with concomitant generation of H_2S, indicating that polymer degradation starts via hydrodesulfurization. Although the decomposition temperature is lower than the one under inert gas, it is still high enough for carrying out various chemoselective hydrogenations described in this work.

Gas-phase hydrogenation of alkynes with various functional groups was carried out with Pd/COP and Pd/γ-Al_2O_3 catalysts in a plug-flow reactor (Table 1). Pd/COP showed generally lower catalytic turnover rates (TOR) than Pd/γ-Al_2O_3 due to the surface poisoning with the sulfur moieties. As shown in reaction 1 with an internal alkyne, a major product on Pd/COP is cis-alkene. This indicates that the hydrogenation takes place via syn-addition of H atoms.[4] In contrast, Pd/γ-Al_2O_3 showed the production of various isomers having different double bond positions and cis/trans geometries (Table 1), indicating that the alkenes can be further isomerized on the unpromoted Pd surface.[44,45] Pd/γ-Al_2O_3 also produced a substantial amount of an overhydrogenated product, octane (15%). Similarly, in reactions 2−3 with the alkynes having C=C and C=O side functional groups, Pd/COP exhibited superior selectivities (85−89%) to corresponding alkenes with minimal hydrogenation of the side functional groups. In contrast, Pd/γ-Al_2O_3 produced substantial amounts of overhydrogenated products (Table 1). In reactions 4−6 with alkynes having cyclopropane, −OH and −NH_2 functional groups, Pd/COP produced predominantly the corresponding alkenes. In contrast, Pd/γ-Al_2O_3 showed more pronounced production of overhydrogenated products and hydrocarbons without cyclopropane ring structure and −OH functional groups (Table 1) due to hydrogenolysis of these functional groups. We also carried out the liquid-phase phenylacetylene (aromatic alkyne) hydrogenation using Pd/COP and Pd/γ-Al_2O_3. Pd/COP showed a significantly higher selectivity (90.5%) for the corresponding alkene (styrene) than Pd/γ-Al_2O_3 (26.2%), that produced a large amount of overhydrogenated product, ethylbenzene (Figure 2). Pd/COP showed excellent recyclability up to five cycles without any substantial loss of activity or selectivity. ICP-MS analysis also confirmed that Pd leaching was negligible
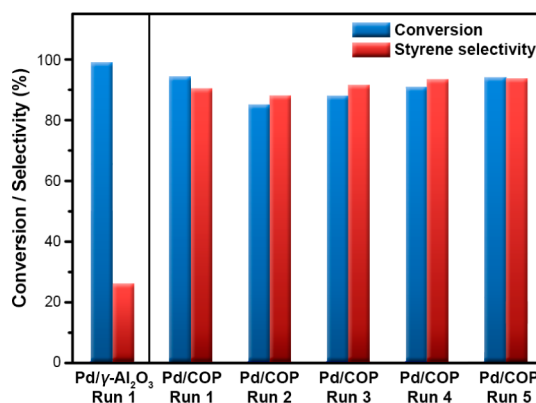
Figure 2. Liquid-phase phenylacetylene hydrogenation with Pd/γ-Al_2O_3 (1 cycle) and Pd/COP (5 cycles) (reaction condition: 1 MPa H_2, 303 K, 5 h reaction).

during the reaction cycles (Pd content was maintained at 1.2 wt %). On the basis of the results, it can be concluded that Pd/COP exhibits superior chemoselectivities in converting alkynes to corresponding alkenes with minimal overhydrogenation, isomerization, and hydrogenolysis of various side functional groups.

To further explore the selective alkyne hydrogenation properties, we investigated acetylene partial hydrogenation in an ethylene-rich feedstock (ethylene/acetylene = 82). The reaction is highly important in industry for removing acetylene impurity from ethylene produced in naphtha crackers.[1,2] For industrial applications, high catalytic selectivity to ethylene over ethane at a very high acetylene conversion level (>99%)[46] is required for minimizing the loss of ethylene. As shown in Figure 3a, Pd/γ-Al_2O_3 showed low selectivity to ethylene (29−56%), and substantial formation of an overhydrogenated
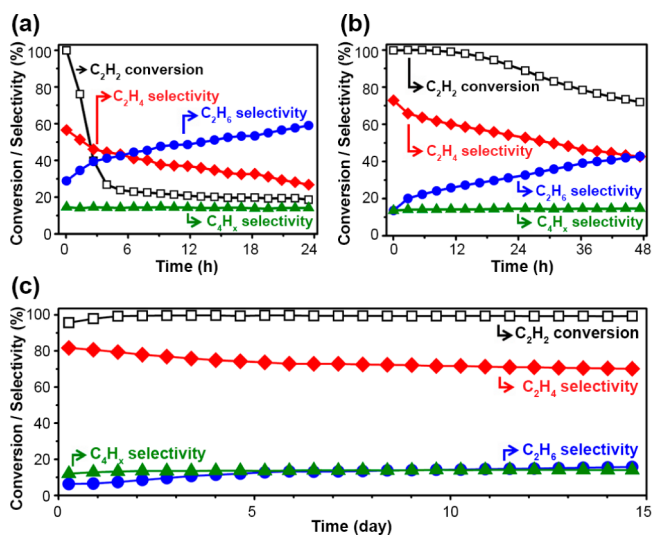
Figure 3. Acetylene conversion and product selectivities as a function of time-on-stream during acetylene hydrogenation in an ethylene-rich stream (reaction condition: 0.6 kPa C_2H_2, 0.6 kPa C_3H_8, 49.3 kPa C_2H_4, 0.9 kPa H_2, and 48.6 kPa N_2 at 393 K). (a) Pd/γ-Al_2O_3, (b) Pd/γ-Al_2O_3 modified with diphenyl sulfide, and (c) Pd/COP. To obtain complete conversion level during the initial reaction period, space velocities of 0.3, 0.04, and 0.02 $mol_{C_2H_2}$ mol_{Pd}^{-1} s^{-1} were used for Pd/γ-Al_2O_3, Pd/γ-Al_2O_3 modified with diphenyl sulfide, and Pd/COP catalyst, respectively.

product, ethane, was detected. Furthermore, the catalytic conversion and ethylene selectivity rapidly decrease with time-on-stream, which is consistent with earlier reports.[1] It was proposed that coke deposits on the catalyst surface can act as an active site for unselective hydrogenation of acetylene to ethane via hydrogen spillover.[1,47] Indeed, after 1 day of reaction, the deactivated catalyst showed substantial coke formation (28 wt % by TGA). In clear contrast, Pd/COP (Figure 3c) showed 70−80% ethylene selectivity even at a complete acetylene conversion level (>99%). Most notably, the catalytic activity and selectivity did not significantly deteriorate over 15 days. Elemental analysis results revealed that Pd/COP contains only 8.4 wt % coke even after 15 days reaction, and the original S/N elemental mass ratio (3.3) did not change significantly (S/N of the fresh catalyst: 3.5). The results strongly support that, despite the organic nature of the COP, the catalyst is thermochemically stable over a long reaction period.

To compare the thermochemical stabilities of the covalently bonded and physically adsorbed modifiers, we impregnated the presynthesized Pd/γ-Al$_2$O$_3$ with 10 wt % diphenyl sulfide as a molecular modifier. The modified Pd/γ-Al$_2$O$_3$ was also tested for acetylene hydrogenation in an ethylene-rich stream (Figure 3b). The catalyst initially showed improved selectivity to ethylene (∼70%) compared with a pristine Pd/γ-Al$_2$O$_3$. However, the catalyst showed a gradual decrease of catalytic activity and selectivity with time-on-stream. The rates of decrease in the catalytic activity and selectivity are much faster than those of Pd/COP. The results strongly support that the physically adsorbed diphenyl sulfide is not stable under the reaction condition. Indeed, TGA analysis confirmed that the physically adsorbed diphenyl sulfide started being leached or decomposed even at 323 K under H$_2$ (Figure S4), which is substantially lower than the decomposition temperature of Pd/COP (503 K). The results indicate that the modifiers covalently bound to a support framework have a significant advantage in terms of thermochemical stability, compared with physically adsorbed modifiers.

From a mechanistic point of view, it is interesting that Pd/COP does not adsorb H$_2$ according to the aforementioned H$_2$ chemisorption experiment (H/Pd ≪ 0.01). This result indicates that Pd/COP lacks H−H dissociation ability because the Pd surface is fully "poisoned" by the sulfur moieties. This is contradictory to the observed alkyne hydrogenation activities, because hydrogenation is generally impossible without H$_2$ activation. A plausible explanation for the reaction mechanism could be obtained from the H$_2$-D$_2$ exchange experiments summarized in Figure 4. Consistent with the chemisorption experiment, H$_2$-D$_2$ exchange does not occur on Pd/COP in the absence of acetylene (Figure 4a). However, in the presence of coflowing acetylene, substantial formation of HD was detected along with ethylene (either nondeuterated or deuterated). The results strongly support that acetylene adsorbs on the Pd surface and enables "cooperative" adsorption of H$_2$ (or D$_2$). In other words, H$_2$ dissociative adsorption is possible only in the presence of acetylene adsorbed on the Pd surface. Notably, coflowing ethylene with H$_2$/D$_2$ did not facilitate H$_2$-D$_2$ exchange, and moreover, ethane formation was negligible (Figure 4b). The results indicated that acetylene, which has a strong interaction with the Pd surface (acetylene binding energy on Pd (111): −136 kJ mol^{-1}),[48] can induce the decapping of the sulfide groups from the Pd surface, while ethylene with weaker adsorption strength (−82 kJ mol^{-1})[48]
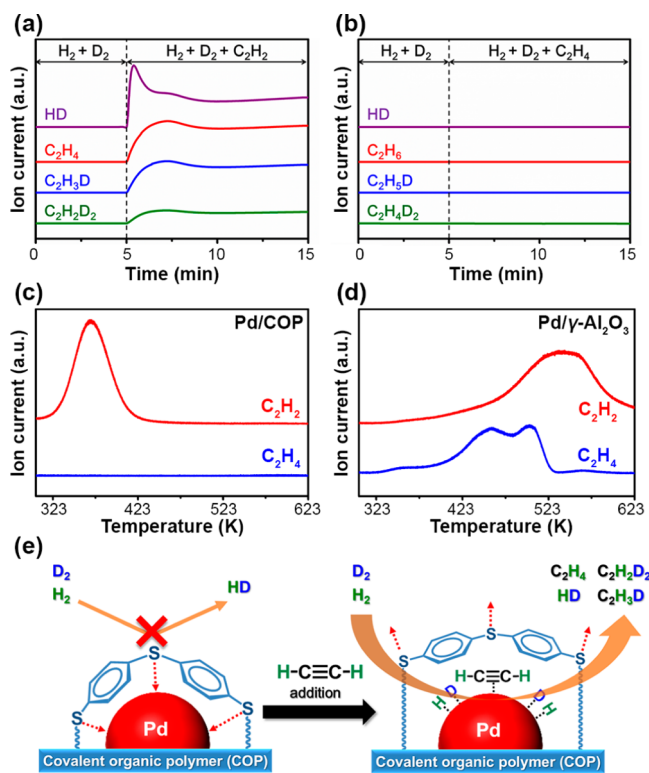

Figure 4. H$_2$−D$_2$ isotope exchange reactions in the presence of coflowing (a) acetylene and (b) ethylene. Temperature-programmed desorption of C$_2$H$_2$ and C$_2$H$_4$ for (c) Pd/COP and (d) Pd/γ-Al$_2$O$_3$ catalysts. The desorption profiles were detected by the mass spectrometer signal at m/z = 15 amu (fragmented C$_1$ species). (e) Schematic explanation of the H$_2$−D$_2$ exchange mechanism on Pd/COP.

cannot. We believe that the binding energy between the sulfur-moieties of COP and Pd is likely to be positioned between those of alkyne and alkene on Pd surface, and thus, only the alkynes with stronger binding energy can be adsorbed on the Pd surface through competitive adsorption. A similar mechanistic role of molecular modifiers was reported by Kwon et al.[25] Temperature-programmed desorption (TPD) experiments with acetylene and ethylene also confirmed that Pd/COP can adsorb acetylene but not ethylene (Figure 4c). In contrast, Pd/γ-Al$_2$O$_3$ showed strong adsorptions of both acetylene and ethylene (Figure 4d). These results infer that the sulfur moieties of the COP ligating the Pd surface act as a "molecular gate" that selectively enables the adsorption of acetylene over ethylene (Figure 4e). It is reasonably expected that the discriminative adsorption behavior would be generally applied for other alkyne/alkene pairs.

■ CONCLUSIONS

In summary, we demonstrated that Pd catalysts supported on a thermochemically stable polymer containing diphenyl sulfide-like moieties (Pd/COP) can be used as a highly chemoselective and long-lived catalyst for partial hydrogenation of various alkynes to alkenes. The exceptionally high alkene production selectivity originated from the distinct adsorption behaviors of the reactant/intermediate on the Pd catalyst surface in the presence of "poisoning" sulfide moieties of the polymer matrix. It is reasonably expected that thermochemically stable polymers containing diverse poison-like functional groups can be used as

versatile catalyst supports to achieve distinct chemoselectivities in various reactions other than the alkyne hydrogenation demonstrated herein. We believe that an optimum compromise between the catalytic activity and selectivity can be achieved in various reactions by rational design of the polymer structure.

■ EXPERIMENTAL SECTION

Catalyst Preparation. A sulfur-containing covalent organic polymer (COP) was synthesized by nucleophilic substitution of cyanuric chloride with 4,4′-thiobisbenzenethiol, following the previously reported procedure after modification.[37] In the synthesis, 5.02 mL of N,N-diisopropylethylamine (DIPEA) was added to 2.16 g of 4,4′-thiobisbenzenethiol dissolved in 220 mL of cyclohexanone. A solution of 1 g of cyanuric chloride dissolved in 40 mL of cyclohexanone was added dropwise into the aforementioned solution with continuous stirring at 273 K in a cooling bath. A white precipitate formed almost immediately. The mixture was further reacted at 303 K for 4 h and at 423 K for 24 h. The solid product was filtered, washed with 600 mL of cyclohexanone, and dried at 373 K for 12 h. Pd (1 wt %) was supported on the COP by conventional wet impregnation of Pd(acac)$_2$ dissolved in tetrahydrofuran (THF). The impregnated sample was dried at 373 K overnight, calcined in dry air (200 mL min^{-1} g^{-1}) at 453 K for 2 h, and reduced in H$_2$ at 453 K (200 mL min^{-1} g^{-1}) for 2 h. A 1 wt % Pd/γ-Al$_2$O$_3$ sample was prepared by impregnating an aqueous solution of PdCl$_2$. PdCl$_2$ (0.1 mmol) dissolved in 0.43 mL of 6.63 M HCl solution was used for 1 g of γ-Al$_2$O$_3$. The impregnated sample was dried at 373 K overnight, calcined in dry air at 573 K for 2 h, and reduced in H$_2$ at 573 K for 2 h. A part of the Pd/γ-Al$_2$O$_3$ sample was modified with 10 wt % diphenyl sulfide by wet impregnation of a hexane solution and drying at 323 K.

Characterization. C, H, N, and S elemental analysis was carried out by using an elemental analyzer, FLASH2000 (Thermo Scientific). Solid-state cross-polarization magic angle spinning (CP/MAS) NMR spectra were obtained at a Larmor frequency, ν_0, of 100.53 MHz for ^{13}C using an Agilent DD2 400 NMR spectrometer equipped with a narrow bore 9.4 T magnet. CP/MAS ^{13}C NMR spectra were recorded with rf-field strength of 30 kHz and recycling delay of 3 s. Chemical shifts were reported in ppm relative to adamantine. N$_2$ adsorption−desorption isotherms were measured using a BEL-Sorp max (BEL Japan) volumetric analyzer at the liquid N$_2$ temperature (77 K) after degassing samples at 423 K for 4 h. Bright-field TEM images were collected by a JEM-2100F (JEOL) at 200 kV. High-angle annular dark-field scanning transmission electron microscopy (HAADF-STEM) images were collected by a Cs-corrected STEM microscope (JEM-ARM200F, JEOL) operating at 200 kV. Particle size distributions were determined by counting more than 300 crystallites. Surface-area-weighted mean cluster diameter was determined using TEM analysis and calculated from $d_{TEM} = \sum n_i d_i^3 / \sum n_i d_i^2$, where n_i is the number of crystallites having a diameter d_i.[49,50] Pd contents of catalysts were determined by inductively coupled plasma mass spectrometer (ICP-MS) using ICP-MS7700S (Agilent). Powder X-ray diffraction (XRD) patterns were recorded using a D/MAX-2500 (RIGAKU) equipped with Cu radiation (40 kV, 300 mA).

X-ray absorption spectra of the Pd K-edge were measured in transmission mode at Pohang Accelerator Laboratory (8C-Nano XAFS beamline). Before the measurements, 0.3 g of a sample was pressurized into self-standing pellets (13 mm diameter) and rereduced at 453 K for Pd/COP and 573 K for

Pd/γ-Al$_2$O$_3$ in in situ XAFS cells equipped with a 0.05 mm thick aluminum window. X-ray photoelectron spectroscopy (XPS) was carried out using a Sigma Probe (Thermo VG Scientific) equipped with a microfocused monochromator X-ray source. The XPS-Pd$_{3d}$ peak was deconvoluted with 2:3 spin−orbit splitting ratios (Δ = 5.26 eV).[39] The binding energies used for the peak deconvolution of XPS-Pd spectra (for 3d$_{5/2}$) were 335.3 eV for metallic Pd (Pd^0)[39] and 337.1 eV for Pd^{2+}−S species,[40] respectively. TGA-MS data were obtained on a thermogravimetric analyzer (TGA N-1500, Scinco) coupled with a quadrupole mass analyzer (Thermostar-GSD 320, Pfeiffer Vacuum). The weight change of the sample and mass spectral data of hydrogen sulfide (m/z = 34 amu) were monitored during a temperature rise from 323 to 773 K with a 5 K min^{-1} heating rate under a H$_2$ flow. H$_2$ chemisorption was performed using an ASAP2020 (Micromeritics) volumetric analyzer at 343 K to avoid the formation of the β-hydride phase.[49] CO chemisorption was performed at 323 K. Prior to the measurements, the samples were rereduced at 453 K for Pd/COP and 573 K for Pd/γ-Al$_2$O$_3$ under a H$_2$ flow. The amounts of chemisorbed hydrogen were determined by extrapolation of the linear region (10−30 kPa) of the isotherm to zero pressure.

Acetylene and ethylene temperature-programmed desorption (TPD) and H$_2$-D$_2$ isotope exchange on Pd/COP catalyst were carried out in a PYREX plug-flow reactor connected to an online mass spectrometer (Thermostar-GSD 320/quadrupole mass analyzer, Pfeiffer Vacuum). Prior to the analysis, 0.5 g of catalyst was rereduced at 453 K under H$_2$ flow. For acetylene and ethylene TPD, rereduced sample was cooled to 303 K, acetylene or ethylene was adsorbed on the sample at 303 K for 3 h, and weakly adsorbed species were removed by purging with He for 1 h at the same temperature. The species that were desorbed from the surface of the catalyst (fragmented C$_1$ species, m/z = 15 amu) were monitored during a temperature rise from 303 to 623 K with 5 K min^{-1} heating rate under He flow. For H$_2$-D$_2$ isotope exchange, rereduced sample was cooled to 393 K and then H$_2$/D$_2$ (1:1 volume ratio) was flowed (60 mL min^{-1} g^{-1}). After 5 min reaction, C$_2$H$_2$ or C$_2$H$_4$ was flowed simultaneously with a H$_2$/D$_2$ mixture (total flow: 100 mL min^{-1} g^{-1}; 40 kPa hydrocarbon, 30 kPa H$_2$, and 30 kPa D$_2$).

Catalytic Measurements. All the gas phase reactions were carried out at atmospheric pressure in a stainless steel plug-flow reactor (10.9 mm diameter) connected to an online gas chromatograph. Catalysts were pelletized, crushed, sieved (150−200 mesh), and then physically mixed with quartz diluents (150−200 mesh). Prior to the reaction, Pd/γ-Al$_2$O$_3$ was rereduced at 573 K and Pd/COP was rereduced at 453 K under H$_2$ flow for 2 h. In order to obtain high alkyne conversion (88−98%), reaction conditions including the space velocity, reaction temperature, and molar ratio of reactant to hydrogen were chosen differently for each reactant. The detailed reaction conditions for each reaction in Table 1 is summarized as follows: (Reaction 1) 1 kPa 4-octyne, 99 kPa H$_2$ at 393 K; space velocity: 0.2 and 3.0 mol$_{4-octyne}$ mol$_{Pd}$$^{-1}$ s^{-1} for Pd/COP and Pd/γ-Al$_2$O$_3$, respectively; (Reaction 2) 1 kPa 1-ethynylcyclohexene, 9 kPa H$_2$, 90 kPa He at 373 K; space velocity: 0.2 and 1.0 mol$_{1-ethynylcyclohexene}$ mol$_{Pd}$$^{-1}$ s^{-1} for Pd/COP and Pd/γ-Al$_2$O$_3$, respectively; (Reaction 3) 1 kPa 3-butyn-2-one, 4 kPa H$_2$, 95 kPa He at 413 K; space velocity: 0.2 and 1.0 mol$_{3-butyn-2-one}$ mol$_{Pd}$$^{-1}$ s^{-1} for Pd/COP and Pd/γ-Al$_2$O$_3$, respectively; (Reaction 4) 1 kPa cyclopropylacetylene, 9 kPa

H_2, 90 kPa He at 363 K; space velocity: 0.2 and 1.0 $mol_{cyclopropylacetylene}$ mol_{Pd}^{-1} s^{-1} for Pd/COP and Pd/γ-Al$_2$O$_3$, respectively; (Reaction 5) 1 kPa propargyl alcohol, 99 kPa H_2 at 393 K; space velocity: 0.2 and 1.0 $mol_{propargyl\ alcohol}$ mol_{Pd}^{-1} s^{-1} for Pd/COP and Pd/γ-Al$_2$O$_3$, respectively; (Reaction 6) 1 kPa propargyl amine, 99 kPa H_2 at 363 K; space velocity: 0.05 and 1.0 $mol_{propargyl\ amine}$ mol_{Pd}^{-1} s^{-1} for Pd/COP and Pd/γ-Al$_2$O$_3$, respectively. Product distributions of Pd/COP and Pd/γ-Al$_2$O$_3$ were compared after 30 min in all reactions.

Liquid-phase hydrogenation of phenylacetylene was performed in a 100 mL Teflon-lined stainless steel autoclave equipped with a magnetic stirrer and a heating jacket. Prior to the reactions, 0.1 g of catalysts was placed in the reactor and rereduced at 373 K under H_2 flow for 1 h. After cooling to 303 K, 4.39 mL (40 mmol) of phenylacetylene, 35 mL of toluene solvent, and 0.65 mL (4 mmol) of octane were added into the reactor. Octane was used as an internal standard. The reaction mixture was stirred (900 rpm) at 303 K under 1 MPa of H_2 for 5 h. After the reaction was completed, the used catalyst was collected by filtration, washed with toluene, and dried at 373 K overnight for recycle test. Recyclability of Pd/COP catalyst was investigated by repetitive reactions up to 5 runs after the prereduction of catalyst. The products were analyzed with a gas chromatograph equipped with a flame ionization detector and a DB-WAX capillary column.

For selective hydrogenation of acetylene in an ethylene-rich stream, a reactant mixture gas containing 0.9% H_2, 0.6% acetylene, 0.6% propane, and 49.3% ethylene in N_2 balance was used. Propane was used as an internal standard. Prior to the reaction, Pd/γ-Al$_2$O$_3$ was rereduced at 573 K. Pd/γ-Al$_2$O$_3$ modified with diphenyl sulfide and Pd/COP were rereduced at 393 and 453 K, respectively, considering the decomposition temperature of organic moieties analyzed by TGA-MS. In the reaction, space velocities of 0.3, 0.04, and 0.02 $mol_{C_2H_2}$ mol_{Pd}^{-1} s^{-1} were used for Pd/γ-Al$_2$O$_3$, Pd/γ-Al$_2$O$_3$ modified with diphenyl sulfide, and Pd/COP catalysts, respectively. The reactant conversion and product selectivities were calculated using the equations given below:[51]

$$C_2H_2\ conversion(\%) = \frac{C_2H_{2_{in}} - C_2H_{2_{out}}}{C_2H_{2_{in}}} \times 100$$

where $C_2H_{2_{in}}$ is the acetylene concentration in the feed before the reaction and $C_2H_{2_{out}}$ is the acetylene concentration in the product stream.

$$C_2H_6\ selectivity(\%) = \frac{C_2H_{6_{out}} - C_2H_{6_{in}}}{C_2H_{2_{in}} - C_2H_{2_{out}}} \times 100$$

where $C_2H_{6_{in}}$ is the ethane concentration in the feed before the reaction and $C_2H_{6_{out}}$ is the ethane concentration in the product stream.

$$C_4H_x\ selectivity(\%) = \frac{2(C_4H_{x_{out}} - C_4H_{x_{in}})}{C_2H_{2_{in}} - C_2H_{2_{out}}} \times 100$$

where $C_4H_{x_{in}}$ is the C$_4$ hydrocarbon concentration in the feed before the reaction and $C_4H_{x_{out}}$ is the C$_4$ hydrocarbon concentration in the product stream. C_4H_x is the sum of the C$_4$ hydrocarbons.

$C_2H_4\ selectivity(\%)$
$$= \left[1 - \frac{(C_2H_{6_{out}} - C_2H_{6_{in}}) + 2(C_4H_{x_{out}} - C_4H_{x_{in}})}{C_2H_{2_{in}} - C_2H_{2_{out}}}\right] \times 100$$

■ ASSOCIATED CONTENT

ⓢ Supporting Information

The Supporting Information is available free of charge on the ACS Publications website at DOI: 10.1021/acscatal.5b02613.

N$_2$ adsorption−desorption isotherm of COP, EXAFS fitting results of the catalysts, XRD patterns of COP and Pd/COP, HAADF-STEM images of Pd/COP, and weight loss of Pd/γ-Al$_2$O$_3$ catalyst modified with diphenyl sulfide during the temperature ramping under H$_2$ (PDF)

■ AUTHOR INFORMATION

Corresponding Author
*E-mail: mkchoi@kaist.ac.kr.

Author Contributions
[#]These authors contributed equally (S.Y. and S.L.).

Notes
The authors declare no competing financial interest.

■ ACKNOWLEDGMENTS

■ REFERENCES

(1) Molnár, Á.; Sárkány, A.; Varga, M. J. Mol. Catal. A: Chem. 2001, 173, 185−221.

(2) Nikolaev, S. A.; Zanaveskin, L. N.; Smirnov, V. V.; Averyanov, V. A.; Zanaveskin, K. L. Russ. Chem. Rev. 2009, 78, 231−247.

(3) Lindlar, H. Helv. Chim. Acta 1952, 35, 446−450.

(4) García-Mota, M.; Gómez-Díaz, J.; Novell-Leruth, G.; Vargas-Fuentes, C.; Bellarosa, L.; Bridier, B.; Pérez-Ramírez, J.; López, N. Theor. Chem. Acc. 2011, 128, 663−673.

(5) López, N.; Vargas-Fuentes, C. Chem. Commun. 2012, 48, 1379−1391.

(6) Kyriakou, G.; Boucher, M. B.; Jewell, A. D.; Lewis, E. A.; Lawton, T. J.; Baber, A. E.; Tierney, H. L.; Flytzani-Stephanopoulos, M.; Sykes, E. C. H. Science 2012, 335, 1209−1212.

(7) Boucher, M. B.; Zugic, B.; Cladaras, G.; Kammert, J.; Marcinkowski, M. D.; Lawton, T. J.; Sykes, E. C. H.; Flytzani-Stephanopoulos, M. Phys. Chem. Chem. Phys. 2013, 15, 12187−12196.

(8) McCue, A. J.; McRitchie, C. J.; Shepherd, A. M.; Anderson, J. A. J. Catal. 2014, 319, 127−135.

(9) Zhang, Q.; Li, J.; Liu, X.; Zhu, Q. Appl. Catal., A 2000, 197, 221−228.

(10) Sheth, P. A.; Neurock, M.; Smith, C. M. J. Phys. Chem. B 2005, 109, 12449−12466.

(11) Pei, G. X.; Liu, X. Y.; Wang, A.; Lee, A. F.; Isaacs, M. A.; Li, L.; Pan, X.; Yang, X.; Wang, X.; Tai, Z.; Wilson, K.; Zhang, T. ACS Catal. 2015, 5, 3717−3725.

(12) Sárkány, A.; Horváth, A.; Beck, A. Appl. Catal., A 2002, 229, 117−125.

(13) Sárkány, A.; Geszti, O.; Sáfrán, G. Appl. Catal., A 2008, 350, 157−163.

(14) Osswald, J.; Kovnir, K.; Armbrüster, M.; Giedigkeit, R.; Jentoft, R. E.; Wild, U.; Grin, Y.; Schlögl, R. *J. Catal.* **2008**, *258*, 219−227.

(15) Armbrüster, M.; Behrens, M.; Cinquini, F.; Föttinger, K.; Grin, Y.; Haghofer, A.; Klötzer, B.; Knop-Gericke, A.; Lorenz, H.; Ota, A.; Penner, S.; Prinz, J.; Rameshan, C.; Révay, Z.; Rosenthal, D.; Rupprechter, G.; Sautet, P.; Schlögl, R.; Shao, L.; Szentmiklósi, L.; Teschner, D.; Torres, D.; Wagner, R.; Widmer, R.; Wowsnick, G. *ChemCatChem* **2012**, *4*, 1048−1063.

(16) Kim, W.-J.; Moon, S. H. *Catal. Today* **2012**, *185*, 2−16.

(17) Teschner, D.; Vass, E.; Hävecker, M.; Zafeiratos, S.; Schnörch, P.; Sauer, H.; Knop-Gericke, A.; Schlögl, R.; Chamam, M.; Wootsch, A.; Canning, A. S.; Gamman, J. J.; Jackson, S. D.; McGregor, J.; Gladden, L. F. *J. Catal.* **2006**, *242*, 26−37.

(18) Teschner, D.; Borsodi, J.; Wootsch, A.; Révay, Z.; Hävecker, M.; Knop-Gericke, A.; Jackson, S. D.; Schlögl, R. *Science* **2008**, *320*, 86−89.

(19) Chan, C. W. A.; Tam, K. Y.; Cookson, J.; Bishop, P.; Tsang, S. C. *Catal. Sci. Technol.* **2011**, *1*, 1584−1592.

(20) Chan, C. W. A.; Mahadi, A. H.; Li, M. M. -J.; Corbos, E. C.; Tang, C.; Jones, G.; Kuo, W. C. H.; Cookson, J.; Brown, C. M.; Bishop, P. T.; Tsang, S. C. E. *Nat. Commun.* **2014**, *5*, 5787.

(21) Vilé, G.; Albani, D.; Nachtegaal, M.; Chen, Z.; Dontsova, D.; Antonietti, M.; López, N.; Pérez-Ramírez, J. *Angew. Chem., Int. Ed.* **2015**, *54*, 11265−11269.

(22) López, N.; Bridier, B.; Pérez-Ramírez, J. *J. Phys. Chem. C* **2008**, *112*, 9346−9350.

(23) García-Mota, M.; Bridier, B.; Pérez-Ramírez, J.; López, N. *J. Catal.* **2010**, *273*, 92−102.

(24) Crespo-Quesada, M.; Dykeman, R. R.; Laurenczy, G.; Dyson, P. J.; Kiwi-Minsker, L. *J. Catal.* **2011**, *279*, 66−74.

(25) Kwon, S. G.; Krylova, G.; Sumer, A.; Schwartz, M. M.; Bunel, E. E.; Marshall, C. L.; Chattopadhyay, S.; Lee, B.; Jellinek, J.; Shevchenko, E. V. *Nano Lett.* **2012**, *12*, 5382−5388.

(26) Long, W.; Brunelli, N. A.; Didas, S. A.; Ping, E. W.; Jones, C. W. *ACS Catal.* **2013**, *3*, 1700−1708.

(27) McKenna, F.-M.; Anderson, J. A. *J. Catal.* **2011**, *281*, 231−240.

(28) McCue, A. J.; Anderson, J. A. *Catal. Sci. Technol.* **2014**, *4*, 272−294.

(29) Vilé, G.; Almora-Barrios, N.; Mitchell, S.; López, N.; Pérez-Ramírez, J. *Chem. - Eur. J.* **2014**, *20*, 5926−5937.

(30) McCue, A. J.; McKenna, F.-M.; Anderson, J. A. *Catal. Sci. Technol.* **2015**, *5*, 2449−2459.

(31) Trimm, D. L.; Liu, I. O. Y.; Cant, N. W. *Appl. Catal., A* **2010**, *374*, 58−64.

(32) Mori, A.; Mizusaki, T.; Miyakawa, Y.; Ohashi, E.; Haga, T.; Maegawa, T.; Monguchi, Y.; Sajiki, H. *Tetrahedron* **2006**, *62*, 11925−11932.

(33) Makosch, M.; Lin, W.-I.; Bumbálek, V.; Sá, J.; Medlin, J. W.; Hungerbühler, K.; van Bokhoven, J. A. *ACS Catal.* **2012**, *2*, 2079−2081.

(34) Xing, R.; Liu, Y.; Wu, H.; Li, X.; He, M.; Wu, P. *Chem. Commun.* **2008**, 6297−6299.

(35) Fujiwara, S.; Takanashi, N.; Nishiyabu, R.; Kubo, Y. *Green Chem.* **2014**, *16*, 3230−3236.

(36) Sun, Q.; Dai, Z.; Meng, X.; Wang, L.; Xiao, F.-S. *ACS Catal.* **2015**, *5*, 4556−4567.

(37) Patel, H. A.; Karadas, F.; Byun, J.; Park, J.; Deniz, E.; Canlier, A.; Jung, Y.; Atilhan, M.; Yavuz, C. T. *Adv. Funct. Mater.* **2013**, *23*, 2270−2276.

(38) Mojet, B. L.; Hoogenraad, M. S.; van Dillen, A. J.; Geus, J. W.; Koningsberger, D. C. *J. Chem. Soc., Faraday Trans.* **1997**, *93*, 4371−4375.

(39) Moulder, J. F., Stickle, W. F., Sobol, P. E., Bomben, K. D. In *Handbook of X-ray photoelectron spectroscopy*; Chastain, J., Ed.; Physical Electronics: Eden Prairie, MN, 1992; pp 118−119.

(40) Hyland, M. M.; Bancroft, G. M. *Geochim. Cosmochim. Acta* **1990**, *54*, 117−130.

(41) Tauster, S. J.; Fung, S. C.; Garten, R. L. *J. Am. Chem. Soc.* **1978**, *100*, 170−175.

(42) Tauster, S. J. *Acc. Chem. Res.* **1987**, *20*, 389−394.

(43) Fu, Q.; Wagner, T. *Surf. Sci. Rep.* **2007**, *62*, 431−498.

(44) Anderson, J. A.; Mellor, J.; Wells, R. P. K. *J. Catal.* **2009**, *261*, 208−216.

(45) Bridier, B.; Pérez-Ramírez, J. *J. Catal.* **2011**, *284*, 165−175.

(46) Jin, Y.; Datye, A. K.; Rightor, E.; Gulotty, R.; Waterman, W.; Smith, M.; Holbrook, M.; Maj, J.; Blackson, J. *J. Catal.* **2001**, *203*, 292−306.

(47) Asplund, S. *J. Catal.* **1996**, *158*, 267−278.

(48) Mei, D.; Neurock, M.; Smith, C. M. *J. Catal.* **2009**, *268*, 181−195.

(49) Choi, M.; Wu, Z.; Iglesia, E. *J. Am. Chem. Soc.* **2010**, *132*, 9129−9137.

(50) Schneider, M.; Duff, D. G.; Mallat, T.; Wildberger, M.; Baiker, A. *J. Catal.* **1994**, *147*, 500−514.

(51) Pachulski, A.; Schödel, R.; Claus, P. *Appl. Catal., A* **2011**, *400*, 14−24.